Available online at www.sciencedirect.com

SciVerse ScienceDirect

Procedia Engineering 00 (2013) 000–000

Procedia Engineering

www.elsevier.com/locate/procedia

The 2014 conference of the International Sports Engineering Association

Flow visualisation experiments on sports balls

James A. Scobie[a]*, Carl M. Sangan[a], Gary D. Lock[a]

[a]*University of Bath, Bath, BA2 7AY, UK*

Abstract

Fluid dynamics plays a significant role in many sports, principally affecting the trajectory of the associated ball. Boundary layer theory can be used to explain why some of these effects take place, demonstrated here for the games of cricket and golf.

The asymmetric nature of a cricket ball, due to the presence of a seam, causes the boundary layer to be tripped into turbulence on one side. On the other hemisphere, the smooth surface promotes laminar flow which separates at a smaller angle relative to the stagnation point. This results in a net pressure force and lateral movement known as swing. In golf inverted dimples are applied to the ball to reduce drag by promoting transition to turbulent flow, this in turn increases the maximum achievable range.

In this study, scaled versions of a smooth sphere, a cricket ball and a golf ball were used to perform wind tunnel experiments in which these fluid dynamic effects were demonstrated. A novel infrared flow visualisation technique, in conjunction with measurements of pressure, highlighted the fluid mechanics at the representative conditions found in each sport. The results underlined the dependence on surface roughness, and provided qualitative visual evidence of the state of the boundary layer at a Reynolds number of 1×10^5.

Selection and peer-review under responsibility of the Centre for Sports Engineering Research, Sheffield Hallam University.

Keywords: Fluid dynamics; flow visualisation; infrared; sports balls

* Corresponding author. Tel.: +44 1225 385939.
E-mail address: j.a.scobie@bath.ac.uk

Selection and peer-review under responsibility of the Centre for Sports Engineering Research, Sheffield Hallam University.

1. Introduction

In the early days of sport, golf balls were made with a smooth surface. It was soon realised, however, that when the surface became worn the ball travelled farther when driven, and subsequently golf balls were manufactured with a dimpled exterior to simulate the effects of wear. In cricket it is a well-established fact that by aligning the seam at a small angle to the flight path, the ball can be made to deviate from its trajectory. The reasons for both these effects can be explained in terms of fluid dynamics and the boundary layer.

Boundary layer flows can exist in two different regimes: laminar and turbulent flow (Prandtl (1904)). In the laminar boundary layer, the layers of fluid slide smoothly over one another and there is little interchange of fluid mass. The turbulent layer has a great deal of fluid-dynamic mixing; this mixing generates a momentum exchange between the high-speed fluid near the edge of the boundary layer and the low speed fluid near the surface. Thus, because it is assisted by the kinetic energy transfused to it from the outside flow, the turbulent boundary layer can flow farther against the adverse pressure gradient than can the laminar layer. Therefore the turbulent layer is said to *stick* to a surface better and remains attached to a sphere further downstream from the stagnation point.

This paper presents measurements of pressure and flow visualisation to demonstrate the state of the boundary layer at a Reynolds number of 1 x 10^5 for a smooth sphere, and scaled models of both a golf and cricket ball (equivalent to 45 mph in cricket and 75 mph in golf).

2. Review of Literature

Achenbach (1972) investigated experimentally the fluid dynamic boundary layer governing the drag coefficient of a hydraulically smooth metal sphere. Figure 1 is reproduced from Achenbach (1972) and (1974) and shows the position of boundary-layer separation obtained from skin-friction measurements. For Re < 2 x 10^5 Achenbach showed that the boundary layer is laminar and separates at 80° . At increased Re, the boundary layer encounters a *critical* condition where the drag coefficient reduces dramatically at Re ≈ 4 x 10^5; here the attached boundary layer is now turbulent and the separation points move downstream to 120°. As the Reynolds number is increased further, the angle of transition translates upstream; the turbulent flow thickens the boundary layer, causing a gradual reduction in the angle of separation (< 120°).

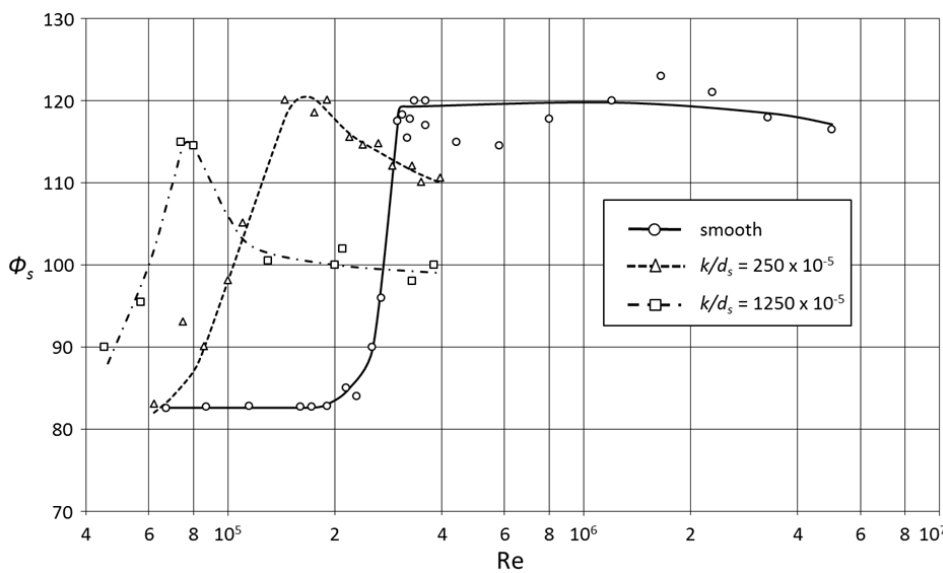

Figure 1: Angle of boundary layer separation (with respect to the stagnation point) plotted against Reynolds number for spheres of differing roughness (Adapted from Achenbach (1974))

Achenbach also investigated the effect of surface roughness on the fluid dynamics of flow around a sphere. As shown in Figure 1, an amount of roughness significantly reduced the critical Reynolds number. The roughness elements disturb the boundary layer, causing transition to turbulence at a lower Reynolds number. The separation angle is a maximum at the *critical* Reynolds number and then significantly decreases as Reynolds number increases.

The fluid dynamics of conventional swing was first explained by Lyttelton (1957). This well-understood phenomenon applies to the new, or well-preserved, ball and has been demonstrated in experiments (see Barton (1982), Bentley *et al.* (1982) and Mehta *et al.* (1983)). Mehta (1985) provides a detailed review of the most significant research performed on baseball, cricket and golf balls with emphasis on experimental results as well as the techniques used to obtain them.

Scobie *et al.* (2013) first introduced the infrared flow visualisation technique presented in this study by demonstrating the fluid dynamics of cricket ball swing. A new theory for why reverse swing, i.e. movement in the opposite direction to conventional swing, occurs at high bowling speeds was also proposed.

3. Experimental Configuration and Techniques

The experiments discussed within this paper were conducted using stationary balls within a wind tunnel. Three scale models: a smooth sphere, a golf ball and a cricket ball (all of diameter 142 mm), were manufactured from nylon by rapid-prototyping. The golf ball and cricket ball were complete with appropriately scaled dimples and seam to mimic their real life counterparts. The corresponding velocities of each counterpart were determined by applying the concept of dynamic similarity (based on the Reynolds number). The scale models were hollow and equipped with static pressure taps (of 1.65 mm diameter) in one circumferential plane. The static pressures were measured using a Scanivalve® system, which was connected to the taps with flexible polyurethane tubing.

Experiments took place using an open-jet return circuit wind tunnel. The tunnel's circular open-jet test section was 0.77 m in diameter and had a working length of 1.5 m. All measurements were made at a velocity of 10 m/s with the turbulence level estimated at less than 1%.

A novel flow visualisation technique (first demonstrated in Scobie *et al.* (2013)) was implemented, using a heat source and an infrared camera, to capture the boundary layer separation point. As in Figure 2, heated air was injected using a heat gun held at the rear of the ball in a similar manner to which smoke is traditionally used in flow visualization experiments. The heated air is entrained into the separated boundary layer near the surface of the sphere. In the steady state, the heat propagates forward until it is met by the cold mainstream air, provided by the wind tunnel, at the separation point. An infrared camera was used to capture thermal images of the surfaces. The flow visualisation technique used here is qualitative, rather than quantitative, as there is a competing mechanism between upstream heat conduction along the surface and convective cooling. Ideally, the surface of the ball would be perfectly insulating; the double-sized ball used here is made of nylon, which is not a perfect insulator and therefore the separation points can only be determined approximately. Although not presented here, pressure measurements were made with and without the heat gun present, confirming that the secondary flow had no influence on the fluid dynamics over the surface of the spheres.

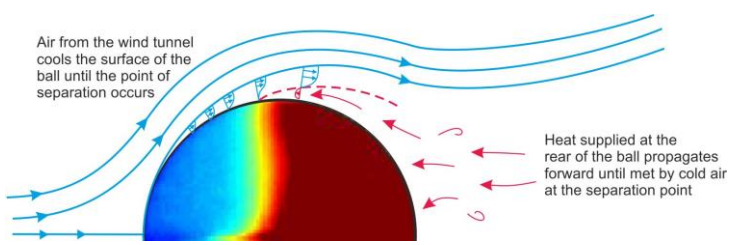

Figure 2: Infrared Flow visualisation technique implemented during the study

The infrared camera used to capture the thermal images was of vanadium oxide Micro-Bolometer Array (MBA) type. It had a sensitivity of less than 85NEdTt1 and a focal length of 11mm.

4. Results

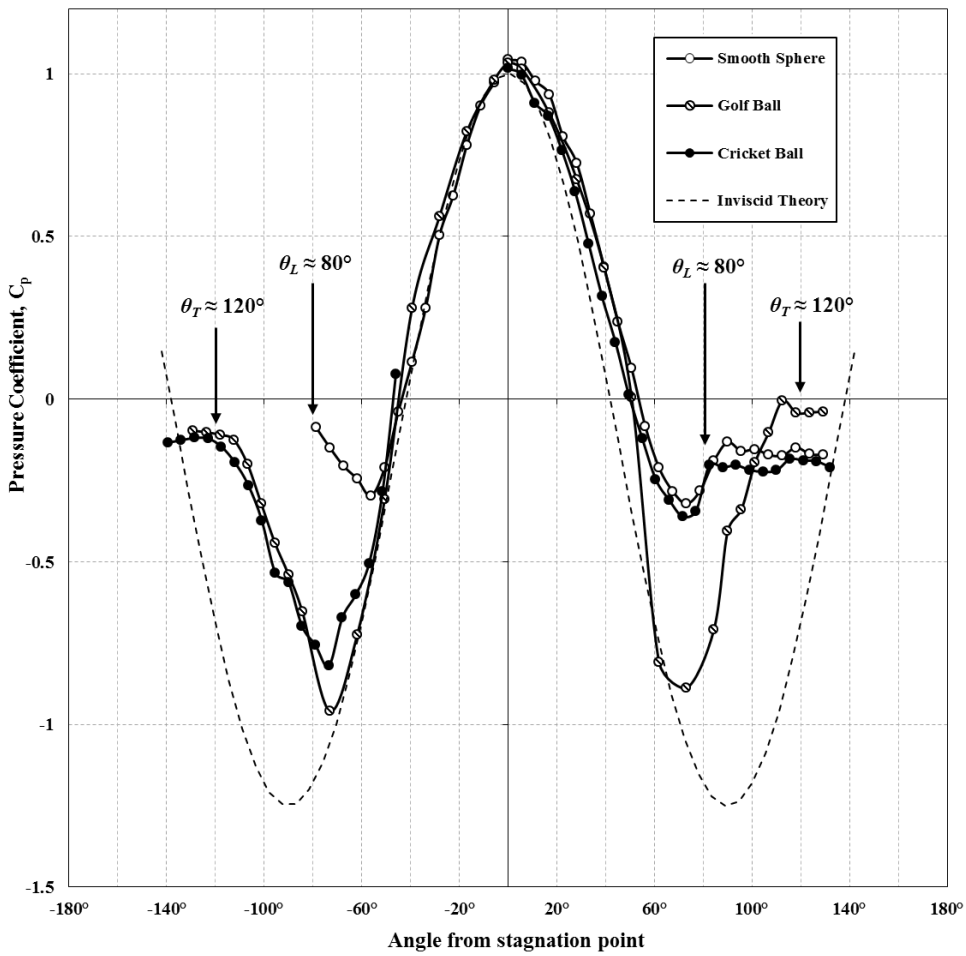

Figure 3: Variation of pressure coefficient with angle from the stagnation point for all models

Figure 3 illustrates the variation of pressure coefficient, ($C_p = (p - p_\infty)/(\frac{1}{2} \rho v_\infty^2)$), with angle from the stagnation point for the three different spheres, each tested at a Reynolds number of 1 x 10^5. Also shown is the pressure distribution expected for an inviscid fluid where there is no flow separation. The constant pressure region at the rear of each sphere on both sides is an indication of separated flow. The angle of boundary-layer separation is indicated by the end of the rise in pressure (i.e. the adverse pressure gradient) to this constant level.

The temperature distributions at Re = 1 x10^5 for the smooth sphere, golf ball and cricket ball models are shown in Figures 4-6 respectively. As discussed above, the flow visualisation provides *qualitative* evidence of the angle of boundary layer separation. Red in the thermal images indicates the regions where the flow is not attached, that is, the boundary layer has separated from the surface of the ball. Conversely, blue indicates that the cool air from the mainstream is attached to the surface. The expected fluid dynamic boundary layer (exaggerated for clarity) is superimposed on each image.

Consider first the smooth sphere. The pressure distribution in Figure 3 is symmetric with laminar separation occurring at approximately 80° from the stagnation point on both sides. This is consistent with the results of Achenbach (highlighted in Figure 1) who showed separation for a smooth sphere occurred at 83° for a Reynolds number of 1 x 10^5. The flow visualisation in Figure 4 demonstrates this laminar separation and diagrammatically indicates the resulting large symmetrical wake.

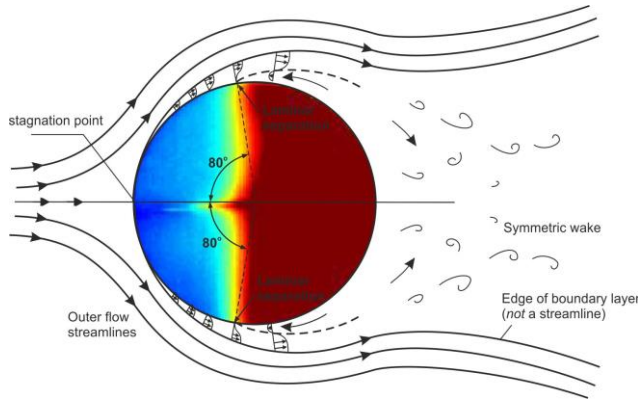

Figure 4: Flow visualisation with superimposed boundary layer for smooth sphere

The pressure distribution for the golf ball model in Figure 3 and the flow visualisation in Figure 5 demonstrates completely different fluid dynamic behavior to the smooth sphere. Flow separation can be seen to occur on both hemispheres of the ball at an angle between 110 and 120°. The dimples on the model roughen the surface and promote transition from laminar to turbulent flow. The boundary layer is therefore better able to withstand the adverse pressure gradient, and so the separation point moves downstream. The consequence is a narrower symmetrical wake as indicated by the streamlines in Figure 5, resulting in a reduction in drag. A roughened golf ball therefore experiences a smaller decelerating force compared with a smooth sphere and consequently would have an increased range. This reduction in drag force is also observable from the Fig. 3; the golf ball pressure distribution plateaus after separation at a smaller negative value in comparison with the smooth sphere. This results in a weaker suction force at the rear, or pressure drag.

Once again with reference to Figure 1, it can be seen that increasing the surface roughness reduces the critical Reynolds number at which a transition from laminar to turbulent flow occurs. It is evident that the separation angle is therefore dependent on both the magnitude of this roughness (k/d_s value) and Reynolds number. The golf ball model had a k/d_s value of roughly 800 x 10^{-5}. At Re = 1 x 10^5, turbulent separation will occur for a sphere of this roughness at an angle of 120°, which is consistent with the pressure measurement and flow visualisation results.

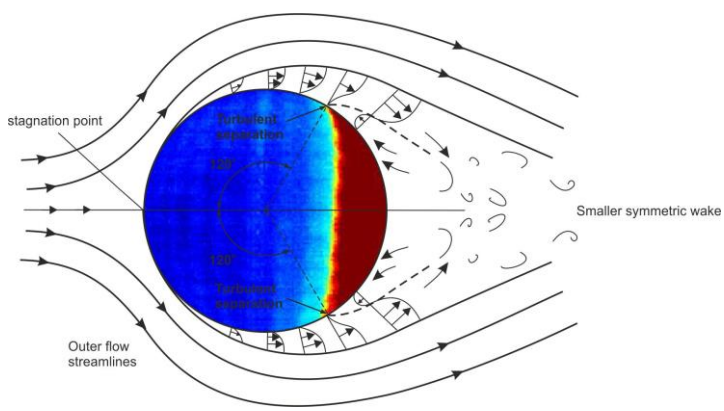

Figure 5: Flow visualisation with superimposed boundary layer for golf ball model

The asymmetric cricket ball demonstrates both laminar and turbulent flow separation on each of its two sides. The seam was inclined at an angle of 15° to the airflow in order to set up a seam and non-seam sides as demonstrated by the polar view (i.e. from above) presented in Figure 6. A Reynolds number of 1 x 10^5 is the equivalent of 44 mph for a real sized cricket ball. This speed is within ranged expect for conventional swing to take place, as confirmed by side force measurements presented in Scobie *et al.* (2013).

The pressure distribution of the non-seam side, shown on the right of Figure 3, behaves in the same manner as the smooth sphere and results in laminar separation at around 80°. The flow passing over the seam side is tripped to turbulent flow by the seam, delaying separation to 120°. The separation angles are captured by the flow visualisation in Figure 6 which highlights a skewed asymmetric wake. The result is a lower pressure on the seam side which creates a net side force and therefore movement of the ball in the direction shown. This is the mechanism which bowlers exploit in order to deceive batmen through swing of a cricket ball.

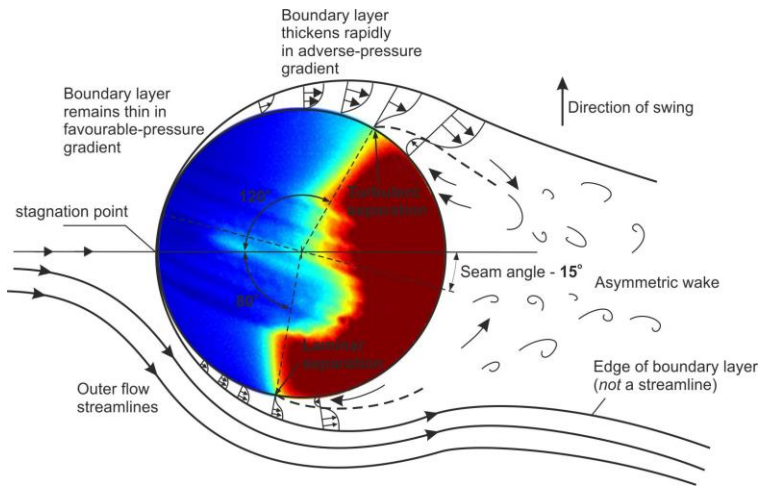

Figure 6: Flow visualisation with superimposed boundary layer for cricket ball model

5. Conclusions

This paper demonstrates the fluid dynamics of the flow around a smooth sphere, golf ball and cricket ball models. A novel method of flow visualisation (using an infrared technique), used in conjunction with pressure measurements, captured the fluid mechanics at a Reynolds number of 1×10^5.

The smooth ball exhibited symmetrical laminar separation at approximately 80° from the stagnation point on both sides. By applying dimples to the model, separation was delayed by promoting transition to turbulent flow. In the context of the game of golf, a dimpled ball will travel further than its smooth equivalent due to the significant reduction in pressure drag.

In cricket, the seam of the ball is exploited by the bowler to create a net transverse pressure force resulting from the asymmetric separation of the fluid dynamic boundary layer on the two sides. On the seam side of the ball, the boundary layer is tripped into turbulent flow and remains attached to an angle of 120°; the flow on the other side of the ball separates in the same manner the smooth sphere at an angle of 80° as there is no seam to trip the laminar boundary layer.

References

Achenbach, E., 1972. Experiments on the flow past spheres at high Reynolds numbers. J Fluid Mech 54(3), pp. 565–575.

Achenbach, E., 1974. The effects of surface roughness and tunnel blockage on the flow past spheres. J Fluid Mech 65(1), pp. 113–125.

Barton, N.G., 1982. On the swing of a cricket ball in flight. P Roy Soc Lond A Mat 379, pp. 109–131.

Bentley, K., Varty, P., Proudlove, M., 1982. An experimental study of cricket ball swing. Imperial College Aero. Technical note, pp. 82-106.

Lyttelton, R.A., 1957. The swing of a cricket ball. Discovery 18, pp.186–191.

Mehta, R.D., Bentley, K., Proudlove, M., 1983. Factors affecting cricket ball swing. Nature 303, pp. 787–788.

Mehta, R.D., 1985. Aerodynamics of Sports Balls. Annual Review of Fluid Mechanics Vol. 17, pp. 151-189.

Prandtl, L., 1904. Über Flüssigkeitsbewegung bei sehr kleiner reibung [On the motion of fluids of very small viscosity]. In: Verhandlungen des III internationalen Mathematiker- Kongresses (ed A Krazer), pp.484–491. Leipzig, Teubner.

Scobie, J.A., Pickering, S.G., Almond, D.P., Lock, G.D., 2013. Fluid dynamics of cricket ball swing. Proceedings of the Institution of Mechanical Engineers, Part P: Journal of Sports Engineering and Technology 227 (3), pp. 196-208.